

AMIC EDUCATIONAL NEWSLETTER

PEDIATRIC IMAGING

PEDIATRIC MUSCULOSKELETAL ULTRASOUND: A PRACTICAL APPROACH

BY MICHAEL ROGAN, MD

Ultrasound is a great imaging modality for pediatrics. It has several characteristics that are helpful for pediatric imaging: non-ionizing images, real-time capabilities and the ability for parents/care givers to hold the child during the procedure. This article will describe some common and some uncommon pediatric musculoskeletal diseases that can be diagnosed using ultrasound, and hopefully make it easier to create excellent diagnostic images.

High quality MSK ultrasound images usually are obtained using high-frequency (10-15 MHz) linear transducers. Normal anatomy includes fat, fascia, tendons, and cartilage (Image 1). A common artifact in tendons is called anisotropy. Anisotropy occurs when the transducer is not perpendicular to the long axis of the

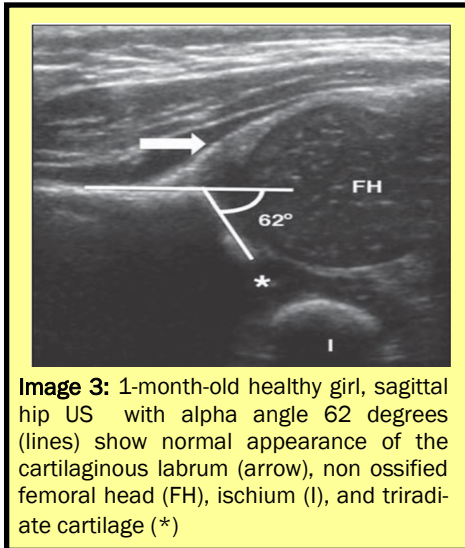


Image 3: 1-month-old healthy girl, sagittal hip US with alpha angle 62 degrees (lines) show normal appearance of the cartilaginous labrum (arrow), non ossified femoral head (FH), ischium (I), and triradiate cartilage (*)

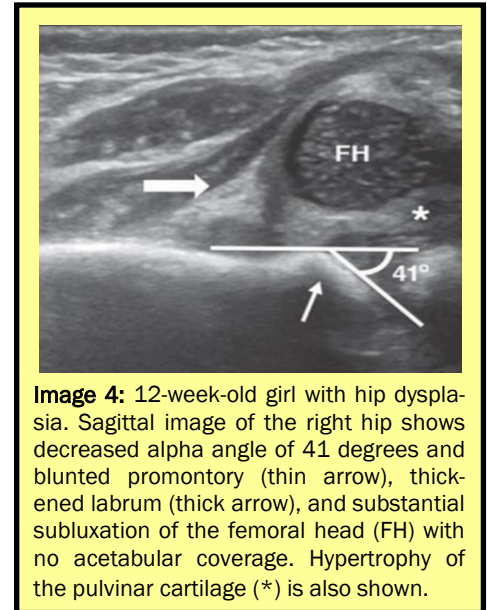


Image 4: 12-week-old girl with hip dysplasia. Sagittal image of the right hip shows decreased alpha angle of 41 degrees and blunted promontory (thin arrow), thickened labrum (thick arrow), and substantial subluxation of the femoral head (FH) with no acetabular coverage. Hypertrophy of the pulvinar cartilage (*) is also shown.

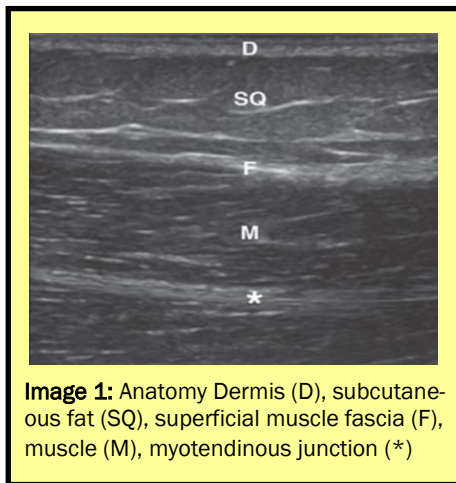


Image 1: Anatomy Dermis (D), subcutaneous fat (SQ), superficial muscle fascia (F), muscle (M), myotendinous junction (*)

tendon, and hypo echoic areas appear which can be incorrectly interpreted as pathology (Image 2).

The most common MSK pediatric exam is the hip ultrasound. Standard images include a coronal and transverse plane. In the coronal plane, the image includes the iliac wing parallel to the transducer, the ischium and the triradiate cartilage. Coverage of the femoral head by the acetabular roof should be greater than 50%, and the alpha angle should be 60 degrees or greater (Image 3). An abnormal hip ultrasound will demonstrate less than 50% coverage of the hip, a shallow alpha angle, or a rounded promontory (Image 4).

Fibromatosis colli is an uncommon cause of congenital muscular torticollis in which a benign fibroblastic proliferation of the sternocleidomastoid muscle leads to thickening and shortening of the muscle. It occurs in infants and is typically noticed by parents who observe the child persistently tilting his or her head to the affected side. Ultrasound is used to diagnose the problem, with images showing heterogeneous and asymmetric fusiform enlargement with or without a focal mass (Image 5). As long as

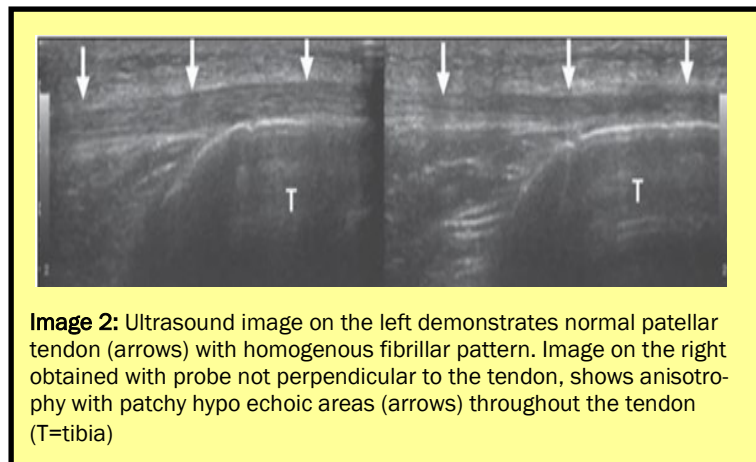


Image 2: Ultrasound image on the left demonstrates normal patellar tendon (arrows) with homogenous fibrillar pattern. Image on the right obtained with probe not perpendicular to the tendon, shows anisotropy with patchy hypo echoic areas (arrows) throughout the tendon (T=tibia)

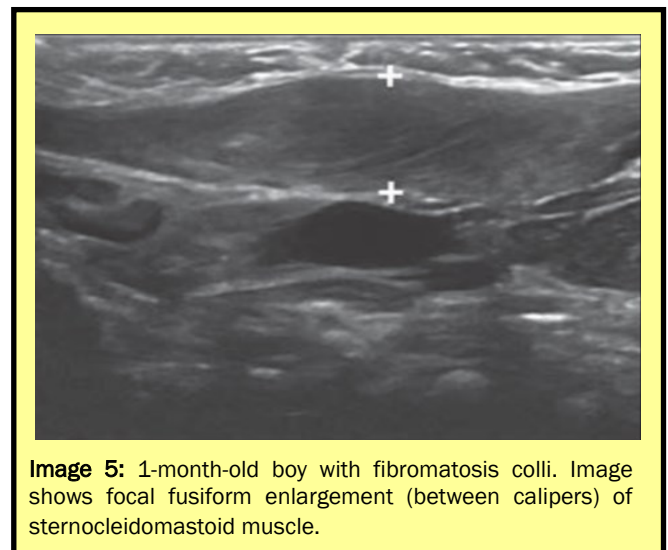


Image 5: 1-month-old boy with fibromatosis colli. Image shows focal fusiform enlargement (between calipers) of sternocleidomastoid muscle.

PEDIATRIC MUSCULOSKELETAL ULTRASOUND CONTINUED...

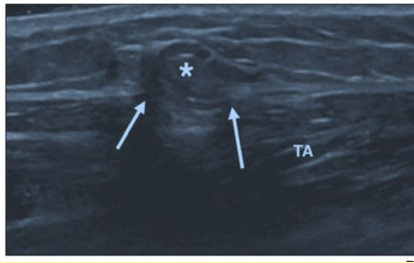


Image 6: 9-year-old boy with painless pretibial bump. US image shows disruption of superficial fascia (between arrows) with focal muscle herniation (*) across fascial plane. TA = tibialis anterior

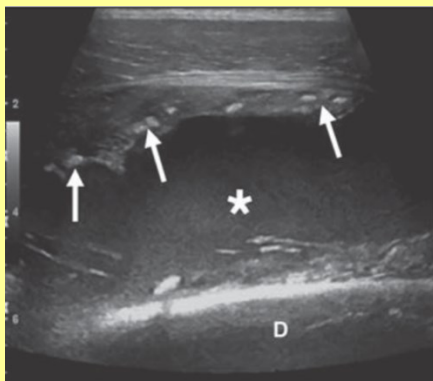


Image 7: 16-year-old girl with myositis ossificans presenting as painful hard lump after recent trauma. Low level echoes are seen (*) overlying femoral diaphysis (D). Small calcifications are seen within the wall (arrows).

surrounding tissue appears normal, an MRI or biopsy is unnecessary.

Muscle hernia is a congenital abnormality which a muscle protrudes through a defect in the investing fascia. This is most commonly seen in the lower extremities, with 70% occurring in the tibialis anterior muscle (Image 6). Because of the dynamic imaging options with ultrasound, the patient can be asked to move the muscle to elicit symptoms and the diagnosis can be confidently made.

Intramuscular hematomas may occur after injuries that mechanically disrupt muscle fibers, and if there is bleeding, the blood may coalesce to form the hematoma. Ultrasound will demonstrate a focal, heterogeneous and avascular collection that displaces the muscle fibers. Ultrasound guided aspiration is associated with decreased pain and quicker return to athletic competition. Post traumatic myositis ossificans can be caused

by a single episode of trauma or multiple episodes at a discrete area. Ultrasound examination of a palpable mass demonstrates an ovoid hypoechoic mass that does not infiltrate adjacent structures. In its early stages, myositis ossificans can demonstrate mild vascularity and ill-defined margins. After the lesion matures, the ultrasound will demonstrate avascularity with an echogenic rim consistent with calcification. Interestingly, 40% of patients will not remember a specific trauma at the site of injury (Image 7).

Ultrasound is a great modality to evaluate for foreign body. If a radiolucent foreign body is suspected (such as a splinter or piece of glass), ultrasound can be used for evaluation. Typically, foreign bodies will be linear and hyper echoic and produce posterior acoustic shadowing (Image 8). Ultrasound can also assist in removing the object

Transient synovitis of the hip is a self-limiting inflammatory condition that is sometimes difficult to separate clinically from the much more serious septic hip. The clinician will describe a patient with hip pain who will not put weight on the affected leg. Ultrasound images are needed to identify fluid in the hip joint, which then can be aspirated using ultrasound guidance (Image 9).

Enlarged lymph nodes are a common finding in children, secondary to infection or inflammation. This finding on clinical exam can cause anxiety in parents and clinicians, as the cause is sometimes unknown. Ultrasound images can sometimes help distinguish lymphadenopathy caused by neoplastic causes from inflammation. A rounded lymph node with an absent fatty hilum is more commonly seen with lymphoma or a bacterial cause, and reactive lymph nodes will typically appear ovoid with a preserved fatty hilum (Image 10). Vascular

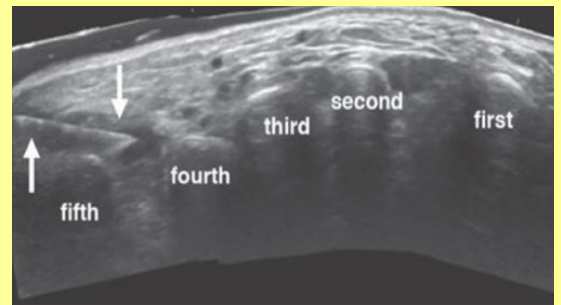


Image 8: 6-year-old girl with foreign body injury to mid-foot. Transverse US image of right plantar mid foot at level of metatarsals (with "first" through "fifth" identifying each metatarsal) shows linear echogenic wooden splinter (arrows) embedded in subcutaneous soft tissues.

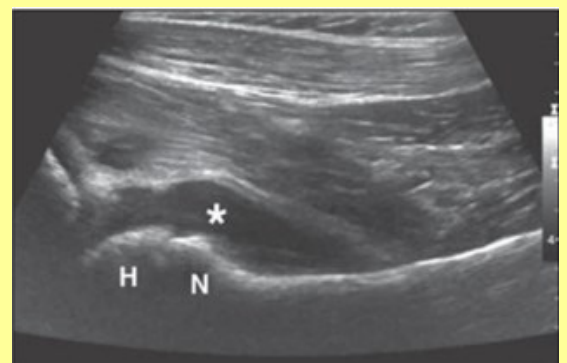


Image 9: 5-year-old girl who presented with limping after having recently had upper respiratory infection. US shows fluid distending the hip joint (*). Patient had toxic synovitis diagnosed. H = femoral head, N = femoral neck.

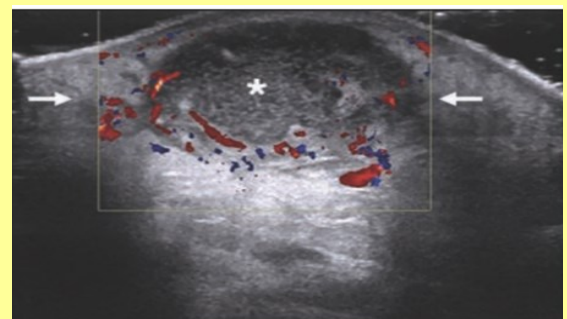


Image 10: 13-year-old girl with suppurative adenitis with painful axillary swelling and erythema. Sagittal color Doppler image of the left axilla shows oval lymph node with heterogeneous parenchyma and peripheral hyperemia (arrows) surrounded by inflammatory change. Swirling internal low level echoes (*) indicate liquification.

PEDIATRIC MUSCULOSKELETAL ULTRASOUND CONTINUED...

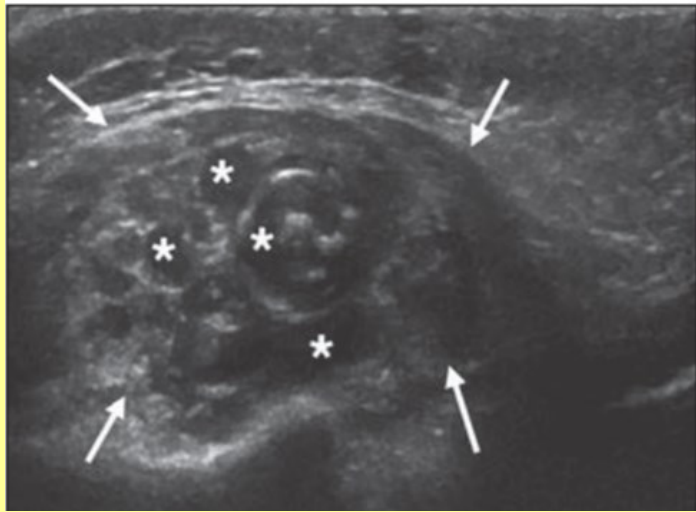


Image 11: 1-year-old boy with lymphatic malformation who presented with painless soft lump on right posterior arm. US image demonstrates a multi loculated cystic mass (arrows) with separations in subcutaneous tissues of the arm. This lymphatic malformation has predominantly macro cystic components (*).

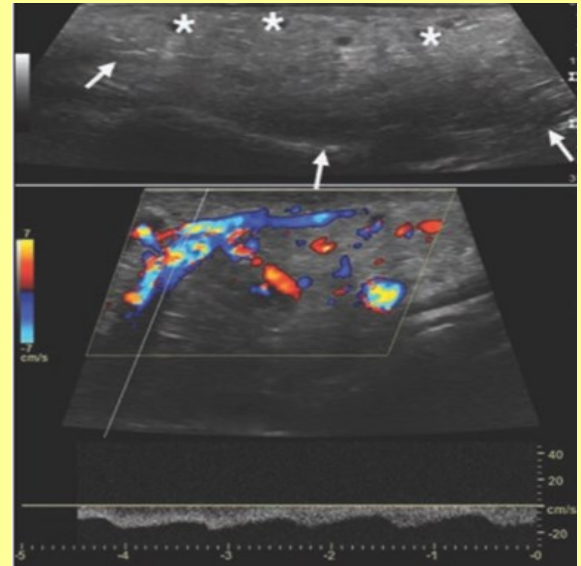


Image 13: 12-year-old girl with arteriovenous malformation with intermittent painful swelling of the cheek. Gray-scale sagittal ultrasound image of abnormal increased echogenicity and thickening in subcutaneous soft tissues. Although this obliterates fat planes of the cheek (arrows), no discrete mass is identified. Few hypo echoic vessels are scattered superficially (*). Spectral sagittal color Doppler image of arteriovenous malformation (bottom) in right cheek shows prominent draining vein with classic arterialized waveform.

malformations are a soft tissue mass that ultrasound can provide a great deal of information about. These are subdivided into lymphatic malformations, venous malformations, and arteriovenous malformations. Lymphatic malformations will appear as multiple cystic spaces with intervening separations (Image 11). Venous malformations typically show a compressible, hypo echoic and heterogeneous lesion (Image 12). Some venous malformations will have phleboliths present. Arteriovenous malformations are

high-flow lesions with shunting because of the absence of a capillary bed. Multiple serpiginous vascular channels are seen with arterial and venous waveforms. Arterialized flow can be seen in the draining veins (Image 13).

As you can see, ultrasound for the pediatric patient can be very helpful. Although imaging the infant hips is the most common type of MSK imaging done, there

Reference:

Hryhorczuk, AL, Restrepo, R, Lee, E. Pediatric Musculoskeletal Ultrasound: Practical Imaging Approach. American Journal of Radiology (AJR): 206, May 2016 W62-W72

Michael Rogan, MD

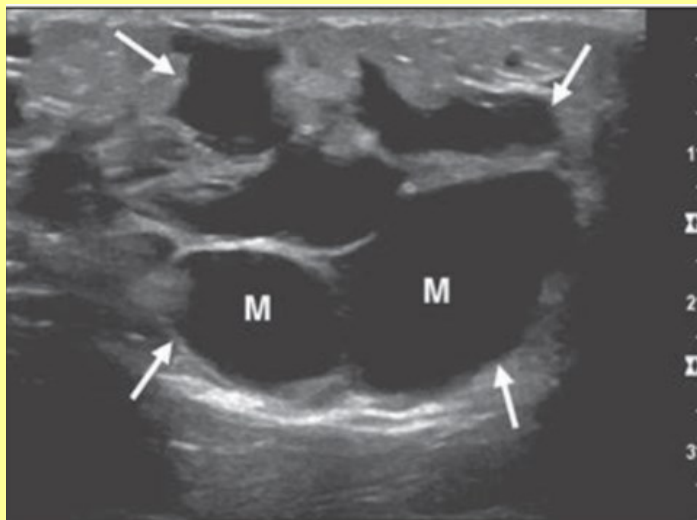


Image 12: 9-year-old boy with venous malformation with painful soft bluish lump in the hand. US image shows well-defined heterogeneous soft-tissue mass (arrows) with anechoic venous channels (M).

are several other differential diagnosis that can be clarified using ultrasound. Hopefully from this article, the reader will have a better understanding of the imaging seen in some of the less common cases that arrive in our radiology department, and with this information the technologist and radiologist will work together to make an accurate diagnosis.



VASCULAR TUMORS/MALFORMATIONS

BY KENNETH CICUTO, MD

In general, vascular abnormalities are divided into binary categories: malformations and vasoproliferative tumors. Simply stated, the latter has increased endothelial cell turnover and the former does not. Malformations are structural abnormalities of the capillary, venous, arterial or lymphatic system that grow in proportion to the child.

Although these can be easy to identify grossly, accurate diagnosis and appropriate treatment are often challenging. Misdiagnosis can lead to delay in appropriate treatment.

Classification has undergone extensive refinement from simple gross description, to the most recent standards of the International Society for the Study of Vascular Anomalies, ISSVS. The society has expanded the system to correlate predictability of clinical history, embryologic origin, disease course and treatment options.



Image 1: Infantile hemangioma.

Vascular tumors:

This category includes infantile hemangiomas, congenital hemangiomas (rapidly involuting and noninvoluting), and more aggressive tumor, i.e. tufted angiomas, Kaposiform hemangioendotheliomas, and angiosarcomas.

Infantile hemangiomas are the most common tumor of infancy and childhood affecting up to 12% of children with a female preponderance. Tumors typically appear between 2 weeks and 2 months of life and follow a proliferating phase, an involuting phase and a state of complete involution (Image 1).

Congenital hemangiomas are tumors that demonstrate intrauterine development with growth completed at birth. These lesions more commonly affect the extremities close to a joint of the head and neck. They are divided into two categories based on biologic activity: rapidly involuting congenital hemangiomas (RICHs) and noninvoluting congenital hemangiomas (NICHs). RICHs typically regress within 6-14 months while NICHs do not regress and have a tendency for progression, usually leading to surgical excision (Image 2).

Kaposiform hemangioendothelioma is a rare vascular neoplasm, which usually arises in the skin and infiltrates into the deeper tissues over time. Most cases are associated with consumptive coagulopathy or Kasabach-Merritt Syndrome, as well as lymphangiomatosis.

Malformation:

Vascular malformations are structural lesions resulting from errors of vascular

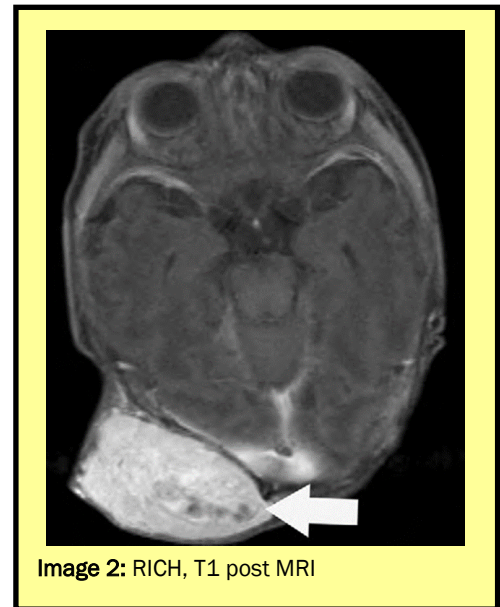


Image 2: RICH, T1 post MRI

morphogenesis. Differentiation of vascular malformations into high flow, low flow or mixed lesions is critical in developing treatment strategies.

Lymphatic malformations arise from abnormal development of the lymphatic system during the early phases of angiogenesis and may be diffuse, often described as lymphedema and previously described as lymphangiomas. These malformations are typically large, spongy masses that are non-tender. These lesions can affect any area of the body, but there is propensity for the head and neck, where they are often referred to as cystic hygromas. 65 to 75% of lesions present at birth whereas the remainder of cases appear with 2 years of age (Image 3).



Image 3: Lymphatic malformation.

VASCULAR TUMORS/MALFORMATIONS CONTINUED...

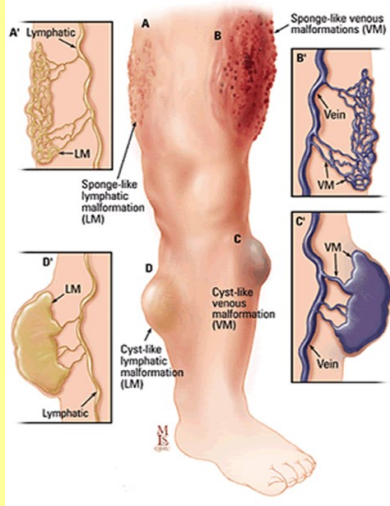


Image 4: Slow flow.

Two thirds of all vascular malformations are venous predominant. Venous malformations result from abnormal sprouting or branching during embryonic development. Venous malformations may be focal, multifocal, diffuse and infiltrative. These dysmorphic vascular channels are lined with flattened endothelium and defective smooth muscle, leading to progressive expansion under hydrostatic pressure. Stasis promotes *in-situ* thrombosis and lysis which presents with swelling and pain, worse as the day progresses and exacerbated in the standing position. Clinically, these lesions appear as a soft, compressible, blue mass typically within the cutaneous tissues of the face, trunk, and limbs (Image 4).

High flow vascular malformations exhibit variable presentation dependent on location. Superficial lesions may present as a warm painless mass with palpable bruit and associated dilated veins. Skin erosion

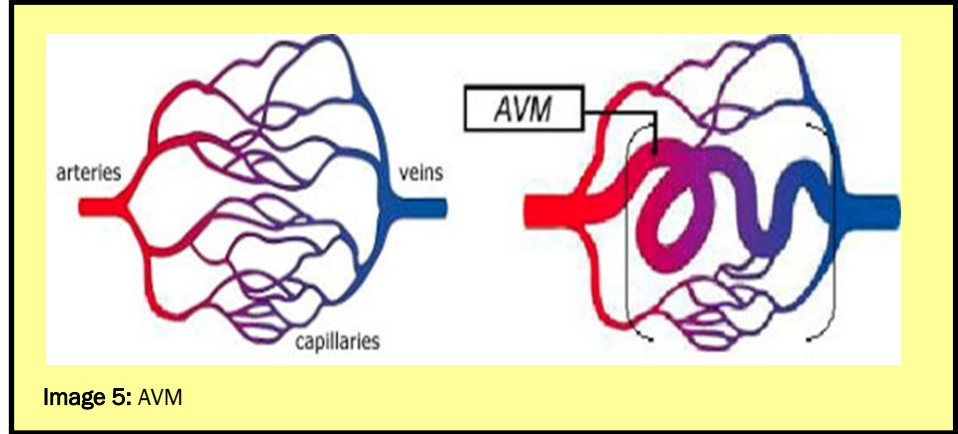


Image 5: AVM

and bleeding is possible. Deeper lesions may present with steal phenomena as the malformation deprives blood flow from downstream structures.

Schrodinger clinical staging system:

- Stage I: A phase of quiescence where there is a cutaneous and skin warmth.
- Stage II: Expansion with a darkening blush, lesion pulsation; a bruit or palpable thrill.
- Stage III: Pain, dystrophic skin changes, ulceration, distal ischemia, and steal.
- Stage IV: Decompensation or high output cardiac failure.

High flow vascular malformations include macrofistulas that consist of single or multiple arteries directly communicating with outflow veins without an interposed high resistance capillary system. In contrast, arteriovenous malformations, which are often extratruncular, consist of a low re-

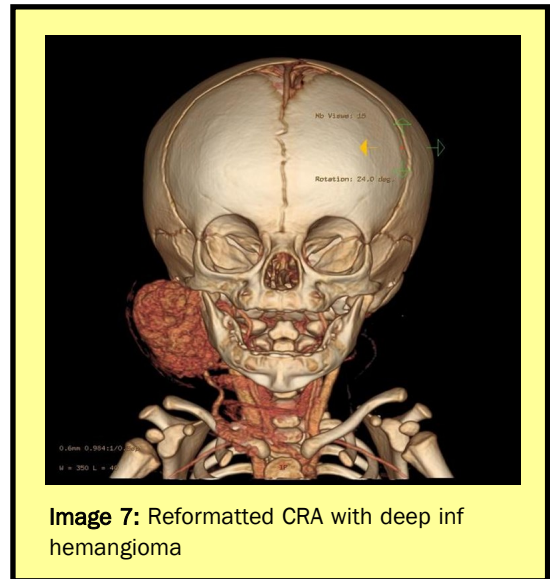


Image 7: Reformatted CRA with deep inf hemangioma

sistance nidus recruiting blood supply from numerous regional inflow arteries and draining by multiple outflow veins (Image 5).

Imaging:

Noninvasive imaging modalities are useful in characterizing vascular anomalies, contributing information about lesion size, flow characteristics and relationship to adjacent structures.

X-ray:

Defining bone and joint involvement and presence of phleboliths. Limitation: vascular classification (Image 6).

CT/CTA:

Enhancement, thrombosis, calcification, vascular anatomy, and involvement of adjacent structures. Limitation: radiation (Image 7).

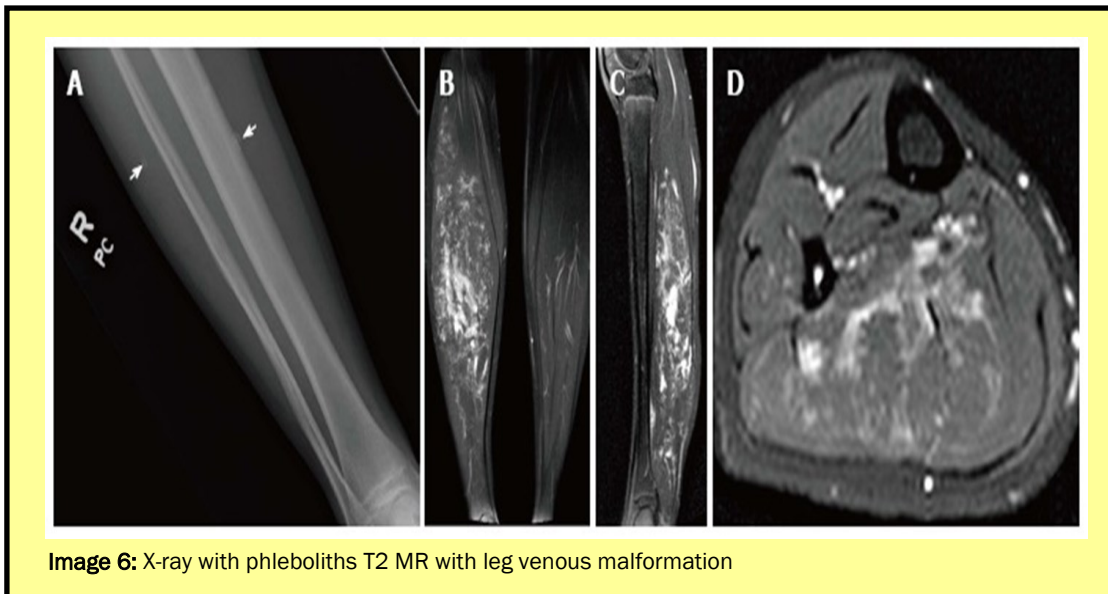


Image 6: X-ray with phleboliths T2 MR with leg venous malformation

VASCULAR TUMORS/MALFORMATIONS CONTINUED...

US:

Low cost, ease of use, high temporal and spatial resolution, and ability to evaluate flow dynamics.

Hemangiomas are reliably differentiated from vascular malformations based on depiction of a well-circumscribed **solid mass**. High-flow vascular malformations, including arteriovenous malformations (AVMs) and arteriovenous fistulae (AVFs), demonstrate arterial and venous waveforms on pulsed Doppler malformations, can be differentiated from high flow lesions based on Doppler analysis. Venous malformations contain enlarged subcutaneous vessels without an associated mass, are compressible and demonstrate venous flow on color and pulsed Doppler US. Lymphatic malformations are characterized by macrocystic or microcystic spaces with or without debris separated by septae. On color and pulsed Doppler US these cyts will contain no flow, however the septa may contain small arteries and veins. Limitations: Deep lesions and bony involvement. (Image 8).

MRI:

MRI is the most valuable modality for imaging vascular anomalies due to its superior contrast resolution, ability to characterize flow dynamics, depiction of deep and adjacent structures, and lack of ionizing radiation.

Hemangiomas will appear as a mass with flow voids and high signal on T1-weighted images, flow voids and high signal on T2-weighted images, high signal within vessels on gradient echo sequences and arterial enhancement on contrast enhanced images.

High-flow vascular malformations including AVMs and AVFs will also demonstrate similar characteristics but no associated soft tissue mass.

Venous malformations will appear as serpentine tubular or amorphous dilated channels containing intermediate signal on T1 weighted images, high signal on T2

weighted images, intermediate signal on gradient echo sequences, and delayed enhancement on dynamic contrast enhanced MRI. Flow voids are not seen within venous malformations due to a lack of fast-flowing blood.

L y m - phatic malformations are characterized by micro/macrocystic spaces that often contain fluid-fluid levels due to hemorrhage or proteinaceous material within the cysts. Cysts will often be hyperintense on T2-weighted images, hypointense on T1 weighted images (though may be iso- to hyperintense depending on proteinaceous contents), and will not enhance. When microcystic, the cystic spaces may not be visible and the fibrovascular stroma seen as regions of intermediate signal on T1-weighted images and high signal on T2-weighted images with associated enhancement on post-contrast images (Image 9).

Treatment:

Lymphatic:

Sclerotherapy is the primary form of treatment of macrocystic lymphatic malformations. Lesions are punctured under ultrasound guidance. The entire contents of the cysts are aspirated and then 25% to 50% of the volume replaced with a sclerosant. Sclerosants include doxycycline, sodium tetradecyl sulfate (Sotradecol, STS), ethanol, bleomycin, and OK-432. Success rates vary from 66-93%.

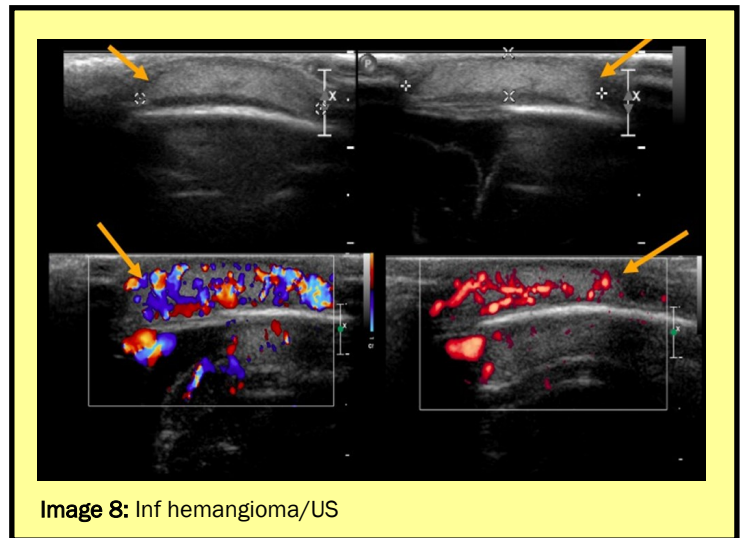


Image 8: Inf hemangioma/US

Low Flow:

Venous malformations may be treated by compression, surgical excision or sclerosis. Treatment is reserved for symptomatic or cosmetically disfiguring malformations. Sclerosing agents, which comprise the main form of treatment, include STS, polidocanol, and absolute alcohol. Recurrence rate is as low as 5% with ETOH.

High Flow:

AV fistulas malformations are treated by coil occlusion of the fistula at the distal arterial end of the communication.

The goal in the treatment of high flow AVM is eradication of the nidus. This is best accomplished with a liquid embolic agent, which will penetrate the feeding vessels into the nidus. A coaxial guiding and microcatheter system is advanced toward the nidus and repeat angiography is performed to determine the volume of embolic agent required to penetrate and fill the nidus. Common agents include n-butyl cyanoacrylate (n-BCA/"glue"), onyx or absolute ETOH.

Kenneth Cicuto, MD

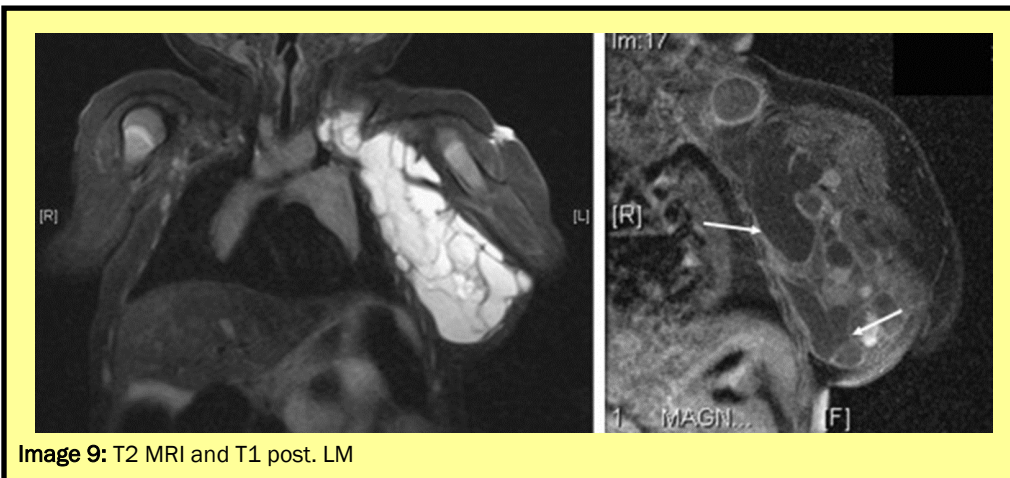


Image 9: T2 MRI and T1 post. LM



CRANIOSYNOSTOSIS: A PEDIATRIC SKULL ANOMALY

BY NICK STATKUS, MD

Infants are born with a malleable skull to allow transit through the birth canal as well as to allow brain growth during development. The cranial sutures are cartilaginous structures which are positioned between the bones of the skull. These remain non-fused during development as the brain grows to allow the skull to enlarge and surround the enlarging brain. The sutures normally begin to fuse when brain growth slows. The premature fusion of the cranial sutures is termed craniosynostosis. The majority of cases of craniosynosto-

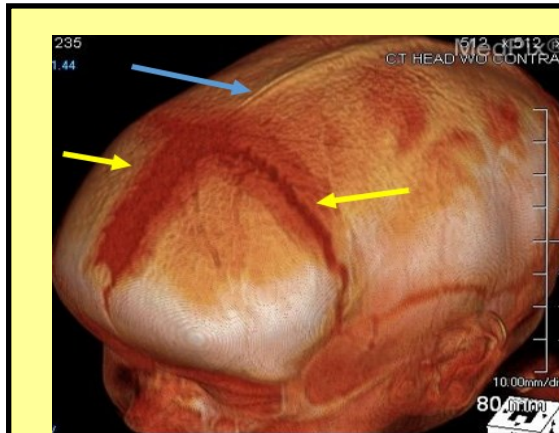


Image 2: 3D head CT reformation shows abnormally fused sagittal suture with a ridged appearance (blue arrow). Compare the abnormal sagittal suture to the metopic and coronal sutures which are open and normal (yellow arrows).

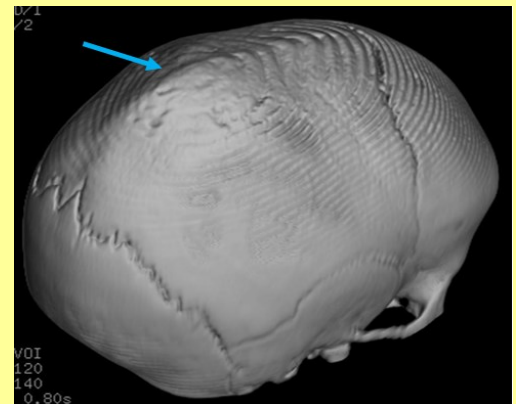


Image 3: 3D head CT reformation shows sagittal suture fusion (blue arrow). Compare the fused sagittal suture to the visible non-fused sutures. A normal sagittal suture would have the same appearance as these non-fused sutures.

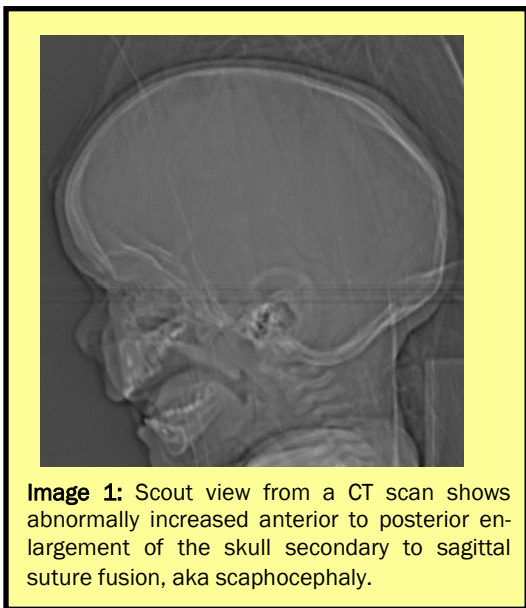


Image 1: Scout view from a CT scan shows abnormally increased anterior to posterior enlargement of the skull secondary to sagittal suture fusion, aka scaphocephaly.

sis occur in isolation (85%) with the minority of cases (15%) occurring in the setting of a congenital syndrome. The pathophysiology and root cause of craniosynostosis is incompletely understood. Fusion of each individual suture results in a characteristic skull deformity which can be seen with visual inspection, physical exam and on imaging studies. Radiographs can be used to diagnose some cases of craniosynostosis, however, the most definitive imaging study is a non-contrast head CT with 3D reformations.

The normal closure of the cranial sutures is highly variable in the population. The metopic suture is the first cranial suture to fuse often by 9 months of age. The sagittal, coronal and lambdoid sutures should be open during the first year of life and fusion of any portion of these sutures during the first year of life is abnormal.

The sagittal suture is the most frequent suture to prematurely fuse with approximately 60% of cases of non-syndromic suture fusion occurring at this site. Early fusion of this suture and its associated skull deformity are termed *scaphocephaly*. The skull exhibits an elongated shape in the AP (anterior-posterior) dimension with fusion of the sagittal suture as the skull grows in the anterior and posterior planes to allow increase in volume for the developing brain (image 1). The suture will either appear fused with bony bridging or may exhibit a ridged appearance on CT (images 2 and 3).

Metopic suture fusion or *trigonocephaly* results in a triangular or wedge-shaped forehead. Fusion of this suture accounts for approximately 15% of cases of non-syndromic suture fusion (images 4 and 5).

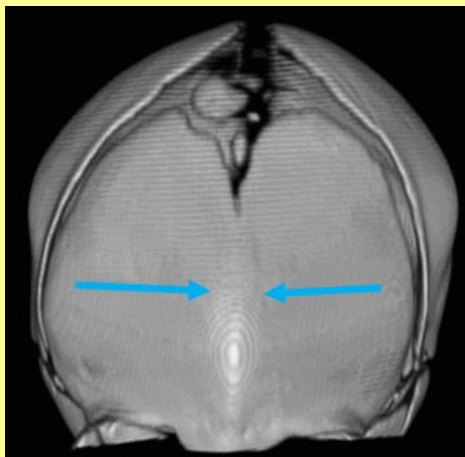


Image 4: Head CT 3D reformation shows fused midline metopic suture with resultant ridged appearance of the midline frontal bone (blue arrows).



Image 5: Axial head CT image shows the triangular shaped frontal bone secondary to metopic suture fusion, aka trigonocephaly (yellow arrows).

CRANIOSYNOSTOSIS CONTINUED...



Image 6: Frontal skull radiograph shows the characteristic uplifting of the ipsilateral orbital roof seen with unilateral coronal suture fusion (blue arrow). Note how it is difficult to see the fused suture on the radiograph. CT is the more sensitive modality to visualize the suture fusion.

Fusion of a unilateral coronal suture accounts for approximately 20% of cases and is termed *frontal plagiocephaly*. Unilateral coronal suture fusion results in the characteristic uplifting of the orbital roof on the affected side resulting in the harlequin deformity (images 6 and 7). Fusion of a lambdoid suture is termed *occipital plagiocephaly* and accounts for approximately 5% of cases. *Plagiocephaly* is a generic term which means flattening of the skull and does not necessarily mean a suture is fused. Occipital plagiocephaly is most commonly a normal finding related to supine positioning of the infant.

References:

1. All pictures courtesy of Medpix imaging archive.
2. Pediatric Neuroimaging. Fourth Edition. A. James Barkovich. Lippincott Williams & Wilkins.

Nicholas Statkus, MD

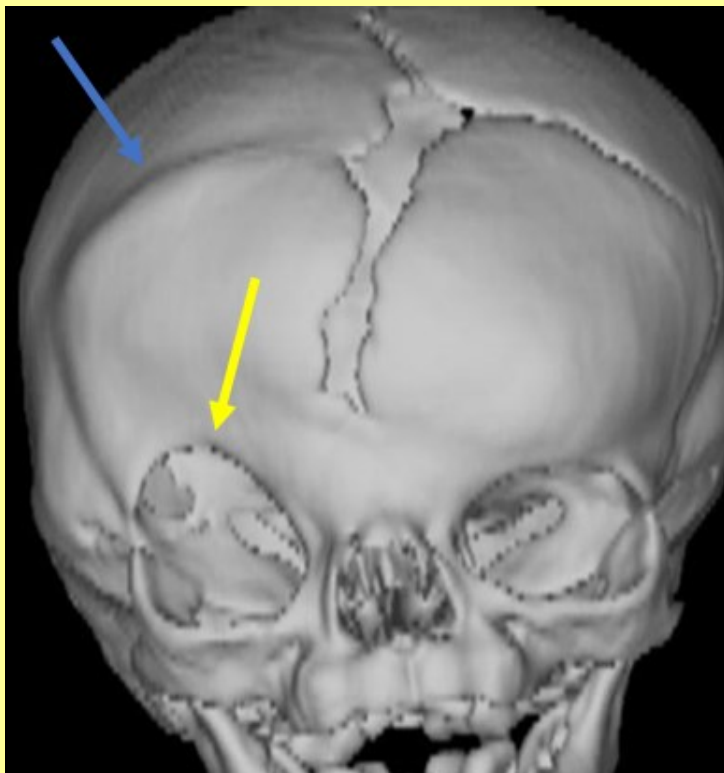


Image 7: Head CT 3D reformation shows right sided unilateral coronal suture fusion with ridged abnormal right coronal suture (blue arrow) as well as uplifting of the ipsilateral orbital roof (yellow arrow), aka the harlequin deformity.

PYLORIC STENOSIS

BY AMY HAYES, MD

Pyloric stenosis, also known as hypertrophic pyloric stenosis or HPS, is a condition in which there is hypertrophy and hyperplasia of the circular muscle of the pylorus and hypertrophy of the underlying mucosa (Image 1).

Pyloric stenosis is relatively common occurring in 2-5 per 1000 live births. It is more common in males (~4:1 male:female) and more common in Caucasians, first born children and children born in younger mothers.

Pathogenesis is not entirely understood. While the etiology remains elusive, a multivariate cause including genetic and environmental exposures is accepted.

occur if the diagnosis is delayed. Parents often report trying several different baby formulas because they (or their physicians) assume vomiting is due to intolerance.

Diagnosis:

On physical exam, an enlarged pylorus, classically described as an "olive," can be pal-

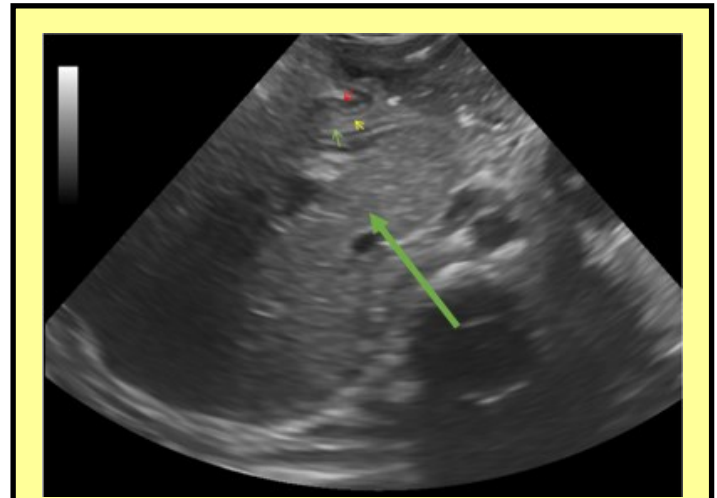


Image 2: Ultrasound image showing the outer anechoic rim (which represents the normal circular muscle) (red arrow), the inner echogenic layer (which represents the mucosa and submucosa) (green arrow) and the inner most anechoic center (which represents fluid in the pyloric canal) (yellow arrow).

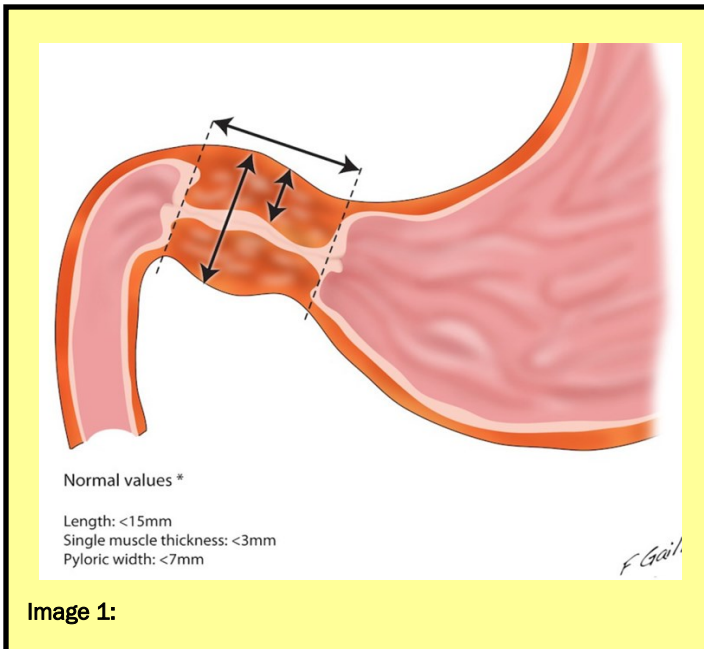


Image 1:

pated in the right upper quadrant or epigastrium of the abdomen in 60-80% of infants. Some studies suggest this is only palpable in 20% of cases so if an olive cannot be palpated it does not exclude the diagnosis.

upper GI may be utilized to make the diagnosis.

Ultrasound:

Images in the long and transverse planes document the hypertrophied pylorus.

Ultrasound criteria for pyloric stenosis are:

- pyloric muscle thickness, i.e. diameter of a single muscular wall on a transverse image: >3 mm (most accurate).
- length, i.e. longitudinal measurement: >15-17 mm
- pyloric transverse diameter: >13 mm

Ultrasound is typically used to confirm or make the diagnosis and if ultrasound is equivocal,

Presentation:

HPS occurs in infants usually in the first 2 months of life and is rare in infants older than 6 months. Typical presentation is onset of initially non-bloody, always nonbilious vomiting at 4-8 weeks of age. Although vomiting may initially be infrequent, over several days it becomes more predictable, occurring at nearly every feeding. Vomiting intensity also increases until pathognomonic projectile vomiting ensues. This is the hallmark of pyloric stenosis.

Patients are usually not ill-looking or febrile; the baby in the early stage of the disease remains hungry and sucks vigorously after episodes of vomiting. Prolonged delay in diagnosis can lead to poor weight gain, malnutrition, and lethargy. Dehydration (with hypochloremic hypokalemic metabolic alkalosis) can

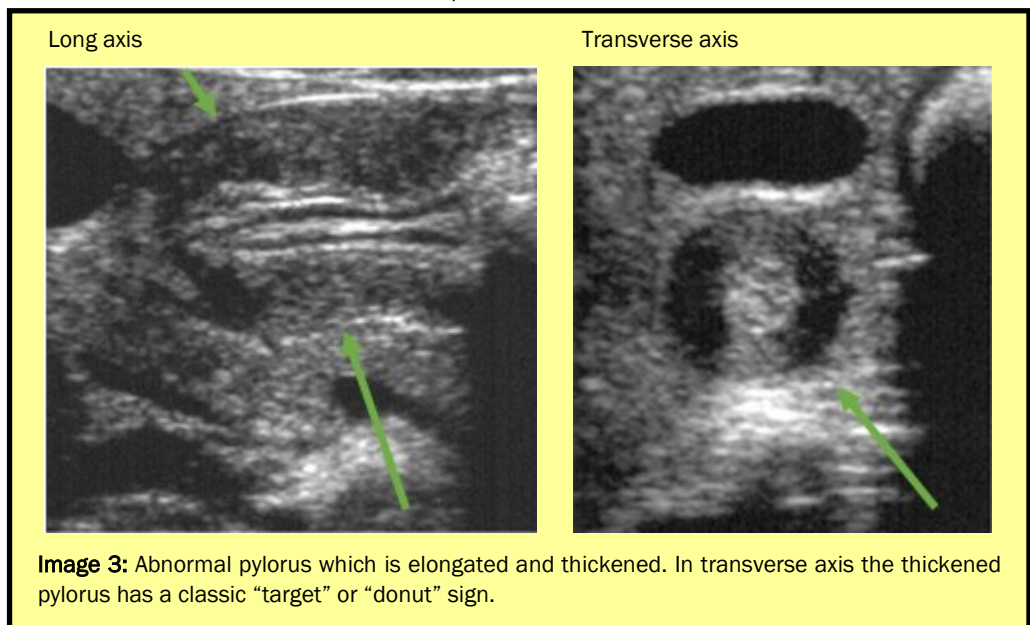


Image 3: Abnormal pylorus which is elongated and thickened. In transverse axis the thickened pylorus has a classic "target" or "donut" sign.

PYLORIC STENOSIS CONTINUED...

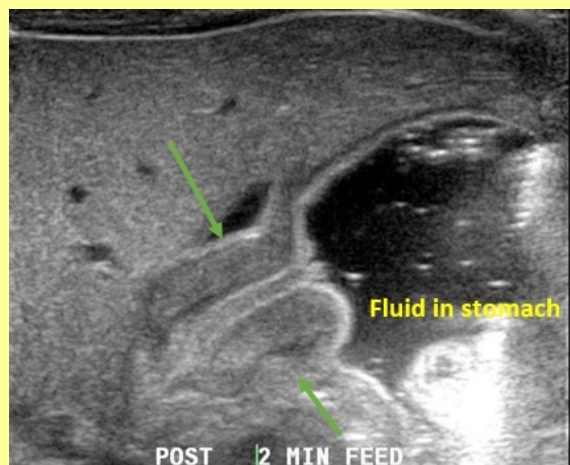


Image 4: Thickened, elongated pylorus with gastric outlet obstruction. Note fluid in the stomach.

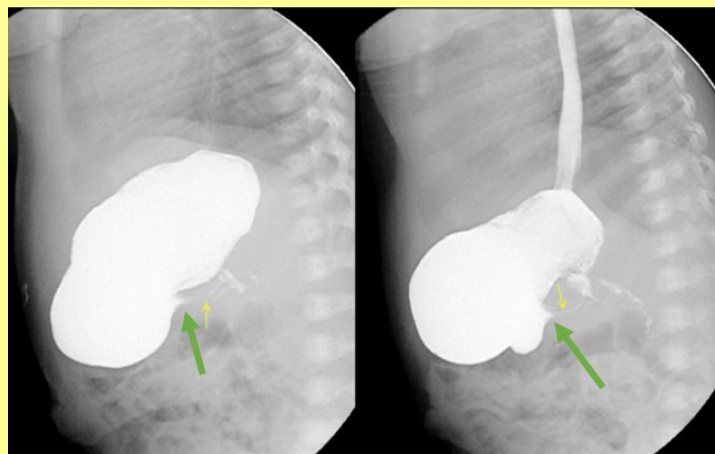


Image 6: Upper GI demonstrating a “double track” sign (yellow arrow). Note that the entrance to the pylorus has a “beak like” appearance (green arrow).

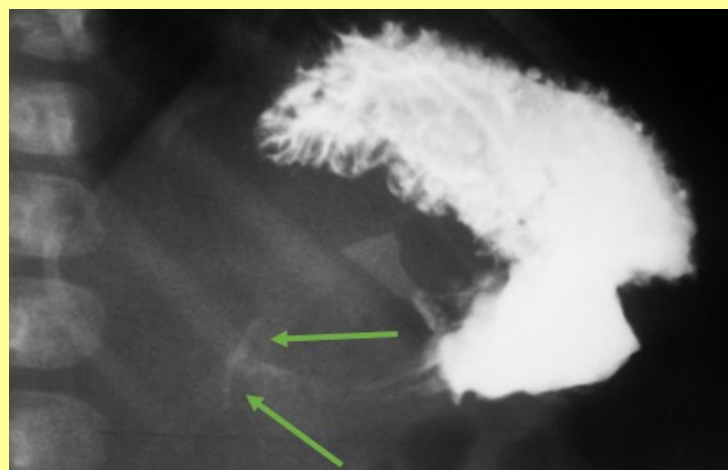


Image 5: “Mushroom sign” - hypertrophied pylorus is indenting the duodenal bulb, giving it a “mushroom” shape.



Image 7: Upper GI demonstrating the “shoulder sign” (yellow arrow) and the “double track” sign (green arrow).

Upper GI can be performed if the ultrasound is equivocal.

Upper GI findings are:

- delayed gastric emptying
- peristaltic waves (caterpillar sign)
- elongated pylorus with a narrow lumen (string sign) which may appear duplicated due to puckering of the mucosa (double-track sign)
- Pylorus indents the contrast-filled antrum (shoulder sign) or base of the duodenal bulb (mushroom sign)
- The entrance to the pylorus may be beak-shaped (beak sign)

Treatment:

Treatment is surgical. The Ramstedt pyloromyotomy is the standard operation. Longitudinal and circular muscles are split. Pylorus returns to normal within 5 months.

Amy Hayes, MD



Advanced Medical Imaging Consultants

Featured Columnists



Michael Rogan, MD

Board-Certified: American Board of Radiology

Fellowship/Subspecialty: Body Imaging, University of Vermont College of Medicine, Burlington, VT
Interventional Radiology, University of Minnesota, Minneapolis, MN

Residency: Diagnostic Radiology, University of Minnesota Medical School, Minneapolis, MN

MD: University of Minnesota Medical School, Minneapolis, MN



Kenneth Cicuto, MD

Board-Certified: American Board of Radiology

Fellowship/Subspecialty: Vascular and Interventional Radiology, Medical College of Wisconsin,
Milwaukee, WI

Residency: Diagnostic Radiology, Maine Medical Center, Portland, ME

MD: St. Louis University School of Medicine, St. Louis, MO



Nick Statkus, MD

Board-Certified: American Board of Radiology

Fellowship/Subspecialty: Neuroradiology, Oregon Health & Science University, Portland, OR

Residency: Oregon Health & Science University, Portland, OR

MD: Oregon Health & Science University, Portland, OR



Amy Hayes, MD

Board-Certified: American College of Radiology

Fellowship/Subspecialty: Vascular & Interventional Radiology, University of New Mexico
Health Science Center, Albuquerque, NM

Residency: Diagnostic Radiology, Virginia Mason Medical Center, Seattle, WA

MD: University of Massachusetts School of Medicine, Worcester, MA